Flow Pattern-Based Modeling of Shell-and-Tube Heat Exchangers with Phase Change for MARS-KS Calculation

Young Seok Bang [a]*, Jungjin Bang [a], Seong-Su Jeon [a], Bub Dong Chung [a], Youngsuk Bang [a]
[a]Future and Challenge Tech. Co. Ltd., Heungdeok1ro 13, Yeongdeok-dong, Giheung-gu, Yongin-si, Gyeonggi-do
[*]Corresponding author: ysbang@fnctech.com

1. Introduction

Nuclear-Renewable Hybrid Energy System (NRHES) is a conceptual system that integrates the nuclear, fossil, renewables, energy storage and industry customers [1]. In the coupling of NRHES to the secondary system of a nuclear power plants (NPP), it is important to evaluate the effect on the secondary system operating parameters caused by the operation of NRHES. Analysis using a software such as PEPSE [2] or Modelica [3] are being attempted for this purpose. PEPSE is a steady-state energy balance software program that calculates the performance of electric generating plants. The Modelica is an object-oriented, equation-based language to model complex physical systems, which can be used for the purpose.

Especially, the validity of the evaluation should be confirmed when those tools are used to evaluate the safety of various transients or accidents that may occur in NRHES or NPP. Calculation using a reliable system thermal-hydraulic code, e. g, MARS-KS [4], can be used for this purpose. It is needed to use the system code to predict the thermal-hydraulic response of major components following the transients of interest, especially heat exchangers which are extensively used in the secondary system. The feedwater heater (FWH) is a typical example of Shell-and-Tube heat exchangers (STHE) and is a special case involving a phase change in the shell-side fluid.

The present paper is to discuss a modeling scheme suitable for predicting the performance of Low Pressure FWH using the MARS-KS code [4]. The problem here is how physically and reasonably the important phenomena such as condensation of the steam supplied to the shell side, the accumulation and distribution of the resulting condensate, and the behavior of drain of the condensate are predicted. This is because excessive or insufficient accumulation of condensed water may cause inaccuracy in predicting the vapor temperature of the shell side, which can eventually lead to inaccuracy of the outlet feedwater temperature of the tube side.

To date, a study among others has been reported that have used system code to model the full scope secondary system [5]. However, in this study, no discussion was made on the effect of the attempted modeling on the behavior of condensate of the shell side and on the feedwater temperature. In the present study, we discuss a modeling scheme based on the actual flow pattern in the shell side. The 'MULTID' component of MARS-KS code is applied to the analysis in order to effectively simulate the behavior of condensate, based on past experiences. Also the distribution and flow of the condensate as well as their impact on feedwater temperature are discussed.

2. Low Pressure Feedwater Heaters (LPFWH)

The details of the design, such as the full length, inner diameter of the shell, number of tubes of the LPFWH are undetermined at the current time. Accordingly, in order to determine the geometric information required for performance analysis, the design process must be performed, starting with the required thermal duty and inlet and outlet conditions. We attempted the basic design by referring to Maarky's LPFWH design [6] for power plants as shown in Figure 1.

Fig. 1. MAARKY Low Pressure Feedwater Heaters

As illustrated in the figure, FWH is generally designed with the concept of three zones, de-superheating, condensing and subcooling as shown in Fig.2.
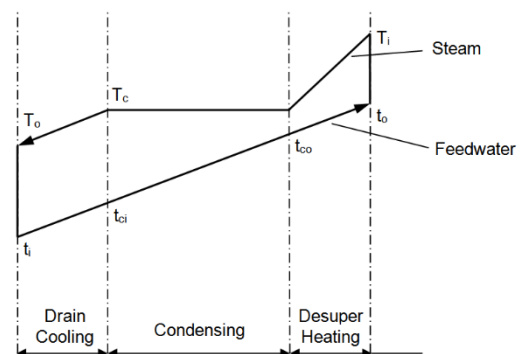

Fig. 2. Design concept of FWH based on three-zone model

In the process of design [7, 8],

1) the heat transfer area required for each zone is determined from the heat load, the log mean temperature difference (LMTD) or arithmetic mean temperature difference (AMTD), and the overall heat transfer coefficient for each zone.
2) From this heat transfer area, the number of tubes is determined assuming the effective tube length and tube diameter.
3) The inner diameter and length of the shell are determined in consideration of the arrangement of the tubes and spatial constraints.
4) The spacing and number of supporting baffles on the shell side suitable for the crossflow flow rate and heat transfer coefficient are determined.
5) Partition plate and baffles to confine the subcooling zone are appropriately determined from the existing FWH database.
6) Geometric data determined by this process is confirmed to be suitable through performance evaluation, or otherwise, it is determined through an additional change process.

In this study, the required heat load and inlet outlet temperatures were from the heat balance diagram at Maximum Guaranteed Rate (MGR) of SSAR of SMART100 design [9]. Although all parts of this design process could not be strictly followed due to many uncertainties, the requested geometric data of LPFWH were determined based on the principles of the design and appropriate engineering assumptions.

In the figure, there is no de-superheating zone and steam flows into the middle point of FWH, but in the present design, the steam injection was placed toward the outlet of the feedwater tube and to what extent the de-superheating area exists. In addition, a partition baffle plate was placed between the subcooling zone and the de-superheating zone to prevent the direct inflow of steam into the subcooling zone. In the future, if detailed information of the LPFWH to be analyzed is provided, those data will be modified.

Table I shows the important design parameters. Figure 2 shows a configuration of the LPFWH to be calculated.

Table I. Design Parameter of LPFWH

Design parameter	Value
Tube side temp. (inlet/outlet), K	316.43/334.43
Shell side temp. (inlet/outlet), K	337.2(339.2*)/322
Heat load required, kJ/s	10,347
Log mean temp. difference, K	4.8
Overall heat transfer coeff. W/m²K	4,000
Required heat transfer area, m²	535.16
Effective tube length, m	6
Tube outer diameter, m	0.01586
Number of tubes/ Tube pitch, m	896/0.005
Tube arrangement	trianglular-60°
Supporting baffle diameter (req), m	0.813
Width of outer gap to shell, m	0.1
Inner diameter of shell, m	1.03
Number/Spacing of baffles,	8/0.667
Partition plate	Baffles 1 ~4
Subcooling zone	Confined

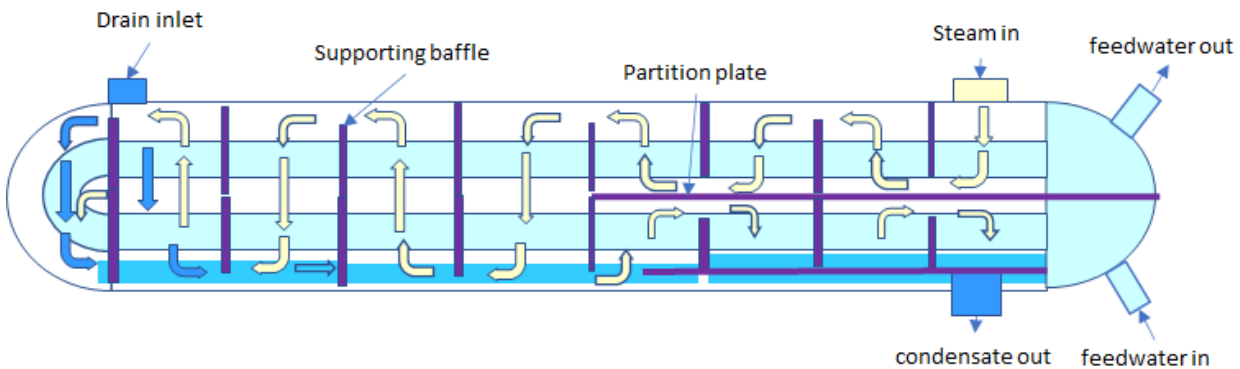Note * temperature of condensate from front-end heaters

Fig. 2. Configuration of LPFWH and shell-side flow pattern

3. MULTID Modeling

Previously, both the tube side and the shell side of LPFWH were approximated using a one-dimensional modeling in the steady-state calculation of whole secondary systems including FWH under the VWO (Valve Wide Open) and MGR conditions,

As a result, it was found that when the shell side is modeled in one-dimensional horizontal flow or a vertical flow, the loss coefficient must be extremely large in order to obtain the required pressure drop between upstream and downstream. In addition, it was confirmed that the application of a loss coefficient of higher than a certain value may cause an excessive accumulation of condensed water locally, resulting in an increase in the amount of saturated water, and in a lower feedwater temperature. Therefore, a modeling scheme was required to avoid the problem of condensed water while

realistically simulating the STHE flow pattern passing through the tube bundle in a crossflow.

MULTID component modeling can be one of the solutions to the concern. Fig. 3 shows a MARS-KS

modeling od LPFWH with MULTID modeling. The important features of this modeling are as follows.
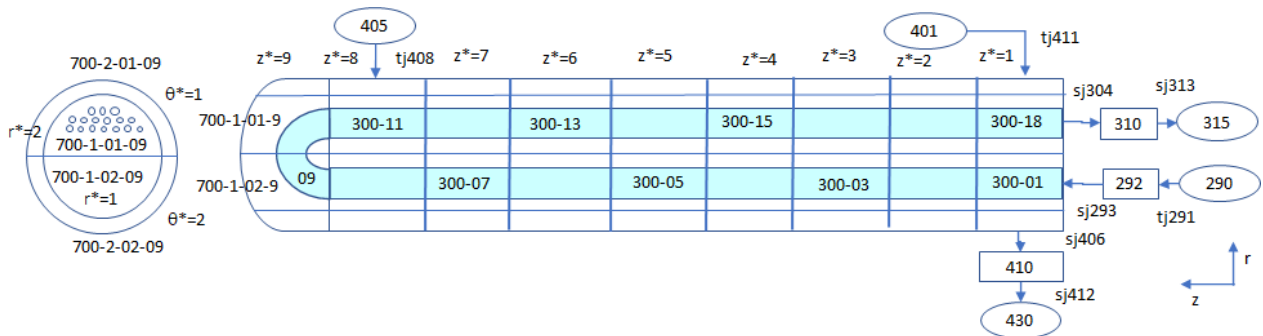

Fig. 3. MARS-KS modeling od LPFWH with MULTID modeling

1) The U tube into which the feedwater flows is modeled by a one-dimensional horizontal pipe component with a total of 18 nodes.

2) The shell part of LPFWH is modeled as a horizontal cylindrical multid component represented by nr=2, nθ=2, and nz=9, and all heat exchanger tubes are located in the cells within the first radius (r*=1).

3) A portion of the upper and lower parts of the shell are separated with a partition plate ($A_{\theta}*=0$, for r*=1, 2, z*=1~4). Where $A_{\theta}*$ and r* denote the fraction of flow area relative to the ideal face area and ring number, respectively.

4) The region designated ad subcooling zone is blocked in radial direction ($A_r*=0$, for r*=1~2, z*=1~4). Inlet to and outlet from the subcooling zone are located at r*=1, z*=4 and r*=1, z*=1, respectively. Where z* means node number in z direction.

5) Cells located within the first radius are blocked in the z direction so that steam can repeatedly flow vertically downward and upward by the supporting segmental baffles ($A_z*=0$ for r*=1, θ*=1, z*=5~9). Where θ* means node number in circumferential direction. However, the cells at the upper part of the condensation zone are slightly open to provide a flow path for steam ($A_z*=0.05$ for r*=2, θ*=1, z*=5~9).

6) Cells located within the second radius are slightly opened in the z-direction alternately so that steam can flow through the baffle-cut of the supporting baffles. ($A_z*=0.2$ for r*=2, θ*=1,2, z*=2,4,6,8)

7) Condensate accumulation may occur in cells without a baffle-cut among cells located at the second radius in the lower half of the shell, so to prevent this, a small opening in the direction z is considered for the junction area. ($A_z*=0.05$ for r*=2, θ*=2, z*=1,3,5,7)

8) The shell-side heat transfer of the U tubes essentially corresponds to the case where the parallel flow and the cross flow coexist with respect to the horizontal tube bundle. In this study, the convection boundary type of 134 (horizontal bundle) was applied as the closest one to this case in the MARS-KS code.

4. Results and Discussion

MARS-KS steady state calculation was conducted with the input implementing the modeling described above. The inlet temperatures and outlet pressures at tube-side and shell-side and flow rate of feedwater shown in Table 1 were imposed as boundary conditions, respectively.
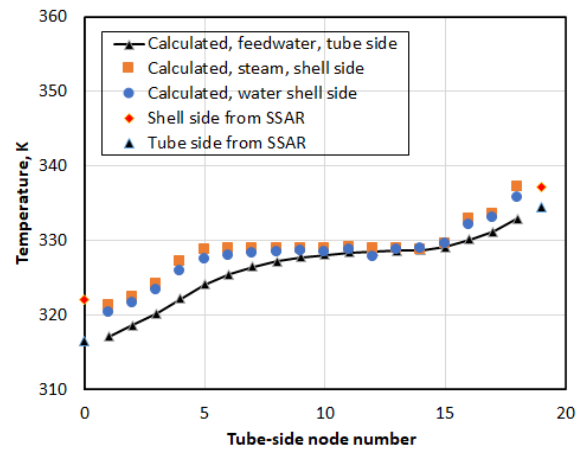

Fig. 4. Temperatures of tube side and shell side

Fig. 4 shows the calculated evolvements of feedwater temperature and shell side temperature. The temperatures at the inlet and the outlet of tube side and shell side from the heat balance of the SSAR were also compared, respectively. From the shell side temperature behavior, three zones can be easily identified. Also the predicted shell temperature are close to the design value. However, the tube outlet temperature was predicted to be slightly lower than the designed value. This means that more improvement in the currently calculated FWH configuration is needed.

Fig. 5 shows the shell side pressures at the cells surrounding the tubes along the tube. The calculation

results generally show a consistent tendency with the temperature distribution, and the pressure drop at the tube inlet side was slightly smaller than the design value.
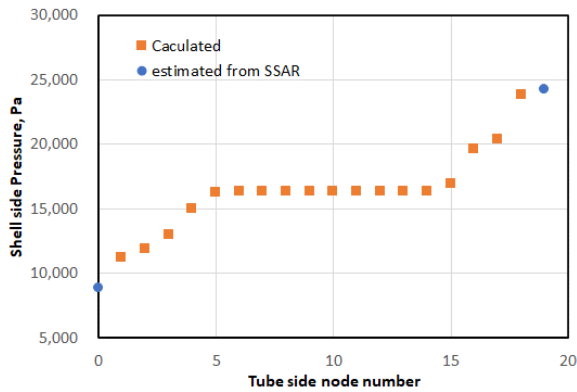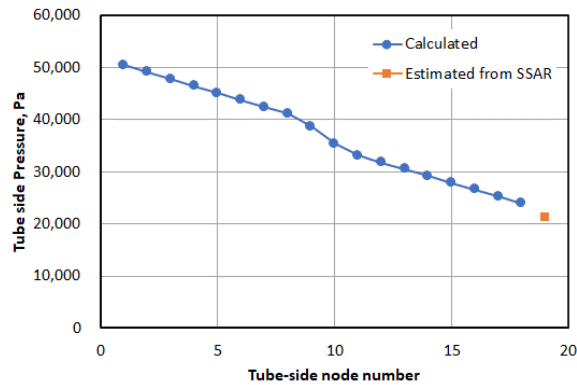

Fig. 5. Shell side pressure

Fig. 6. Tube side pressure

Fig. 6 shows the tube side pressures, which indicates well prediction of pressure drop in tube side.

Fig. 7 shows the calculated liquid fractions at the shell side. Cells having a node number greater than 9 refer to cells on the upper half of the shell.
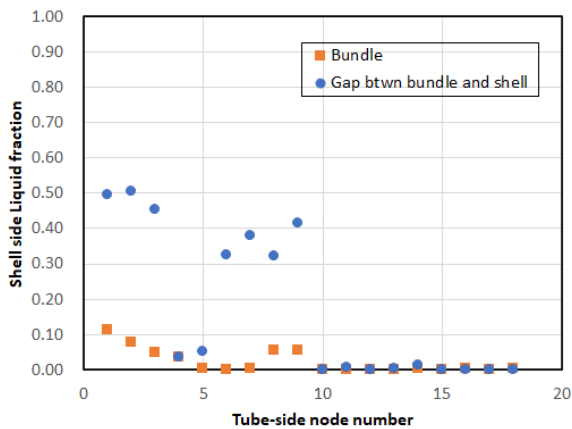

Fig. 7. Liquid fractions in shell side

As shown, those cells show that condensed water flows properly and little accumulation of liquid. Condensate accumulation is found on the lower side of

the shell, but excessive accumulation is not found. In particular, it can be seen that the condensed water generated at the bundle part (node numbers 6 to 10) is properly drained as it flows into the subcooling zone (node numbers 1 to 4). Those prediction results suggest that the current multid modeling is appropriate for simulating the drain of condensate from the upper half and lower half of the shell.

Fig. 8 shows a transient calculation of the step change of steam flow rate injected to the shell side from the 3.6 to 1.6 kg/sec while other parameters are the same.
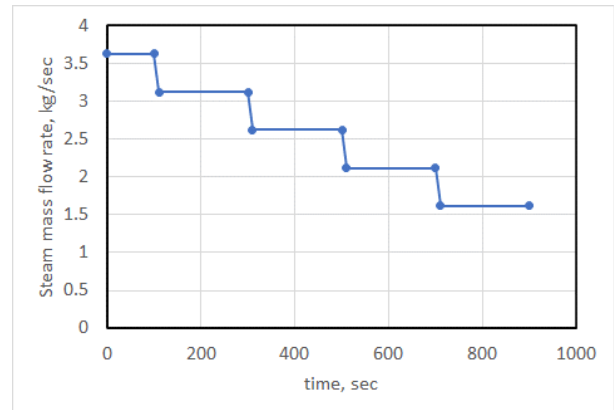

Fig. 8. Step change of steam flow rate

Fig. 9 shows the responsse of the shell side steam temperature and the feedwater temperature induced by the change of steam flow rate. One can find the temperature responses was properly predicted in terms of the timing of the temperature change and the magnitudes of the changes. This fact means that the present MULTID model can appropriately implement the influence of transient where operating conditions are changed.
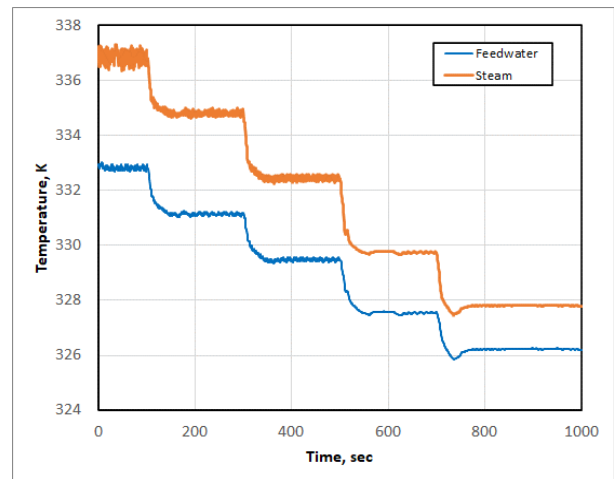

Fig. 9. Response of steam temperature and feedwater temperature

5. Conclusions

The present paper discussed the flow pattern-based MULTID modeling scheme to properly predict the

performance of a shell-and-tube type heat exchanger with phase change using MARS-KS code.

The current MULTID modeling was found appropriate for predicting the feedwater temperature and for simulating the drain of condensate from the upper half and lower half of the shell.

In calculations to date, there have been small differences in outlet temperature on the tube side, outlet pressure on the shell side from those of the SSAR. Those differences are expected to be solved by improving specific geometric information within the MULTID modeling if actual design information is provided.

Also it can be concluded that that the present MULTID model can appropriately implement the influence of transient where operating conditions are changed.

ACKNOWLEDGEMENT

REFERENCES

[1] Y. Bang et al, A Study on Flexibility Modeling of Nuclear-Renewable Hybrid Energy System, Transactions of the Korean Nuclear Society Autumn Meeting Goyang, Korea, October 24-25, 2019.

[2] A. M. Kluba et al, Impact of the Thermal Energy Storage System on APR1400 Turbine, Transactions of the Korean Nuclear Society Virtual Spring Meeting, July 9-10, 2020.

[3] A. M. Kluba et al, APR1400 Secondary Cycle Modeling Integrated with Thermal Energy Storage Using OpenModelica, Transactions of the Korean Nuclear Society Virtual Autumn Meeting, October 21-22, 2021

[4] KINS, MARS-KS Code Manual, Volume II: Input Requirements, KINS/RR-1822, Vol. 2, Daejeon, Korea, 2018.7.

[5] D. Lu et al, Full Scope Modeling and Analysis on the Secondary Circuit of Chinese Large-Capacity Advanced PWR Based on RELAP5 Code, Science and Technology of Nuclear Installations, Volume 2015, Article ID 913274, http://dx.doi.org/10.1155/2015/913274.

[6] Maarky Thermal Systems, Feedwater Heaters, https://maarky.com/products/feedwater-heaters/

[7] Heat Exchanger Institute Inc., Standards for Closed Feedwater Heaters, 9th Edition, 2015.

[8] TEMA, Standards of the Tabular Exchanger Manufacturer Association, 9th Edition, 2007.

[9] KHNP, KAERI, KACARE, SMART100 Standard Safety Analysis Report, 2019.